PHYSICAL REVIEW E **73**, 055302(R) (2006)

Grid states and nonlinear selection in parametrically excited surface waves

T. Epstein and J. Fineberg
The Racah Institute of Physics, The Hebrew University of Jerusalem, Jerusalem 91904, Israel
(Received 11 August 2005; published 12 May 2006)

Interacting surface waves, parametrically excited by two commensurate frequencies (Faraday waves), yield a rich family of nonlinear states, which result from a variety of three-wave resonant interactions. By perturbing the system with a third frequency, we selectively favor different nonlinear wave interactions. Where quadratic nonlinearities are dominant, the only observed patterns correspond to "grid" states. Grid states are superlattices in which two corotated sets of critical wave vectors are spanned by a sublattice whose basis states are linearly stable modes. Specific driving phase combinations govern the selection of different grid states.

DOI: 10.1103/PhysRevE.73.055302 PACS number(s): 47.54.−r, 05.45.Gg, 47.27.Rc, 52.35.Mw

Three-wave interactions are among the most generic types of interactions between nonlinear waves that occur in nature. These are the lowest order (quadratic) nonlinear interactions and, unless barred by symmetry constraints, will generically occur in driven nonlinear systems. Examples range from plasmas and fluids to nonlinear optical systems [1]. As depicted schematically in Fig. 1(a), we consider two sets of critical modes with wave number k_c, that couple quadratically to a third linearly damped mode with wave number k_d, which is not directly introduced by the forcing. We will demonstrate that the only observed nonlinear states are members of an infinite family of "grid" states [2]. Different grid states will be selected by perturbing the system so as to favor a desired linearly damped mode.

Grid states are composed of two sets of hexagonal lattices, $\vec{K}_i^1, \vec{K}_i^2$ (i=1,...,6) where $|\vec{K}_i^{1,2}|=k_c$, that are corotated by an angle θ so as to couple to $k_d=2k_c\sin(\theta/2)$. The defining feature of grid states is that the 12 critical wave numbers lie on a hexagonal sublattice spanned by basis vectors, $\vec{k}_{grid_{1,2}}$ [Fig. 1(b)]. n_1 and n_2 are coprime integers such that $\vec{K}_1^1=n_1\vec{k}_{grid_1}+n_2\vec{k}_{grid_2}$ and $\vec{K}_1^2=n_1\vec{k}_{grid_1}+(n_1-n_2)\vec{k}_{grid_2}$, with the remainder of the $K_i^{1,2}$ obtained by $\pi/3$ rotations.

We label each grid state by the integers $n_1:n_2$ needed to span the state, where $n_1>n_2>\frac{1}{2}n_1>0$, and n_1+n_2 is not a multiple of 3. These yield rotation angles, θ, and basis vectors, k_{grid}, given by [2]

$$\cos(\theta)=\frac{n_1^2+2n_1n_2-2n_2^2}{2(n_1^2-n_1n_2+n_2^2)}, \tag{1}$$

$$k_{grid}=k_c/\sqrt{n_1^2-n_1n_2+n_2^2}. \tag{2}$$

The damped mode, k_d, can either coincide with k_{grid} or be, itself, a linear combination of $\vec{k}_{grid_{1,2}}$.

To date, only one type of grid state, $n_1:n_2=3:2$ ($\theta=22°$), has been identified experimentally [3,4] in the Faraday system. Although not identified as such, candidates for grid states have also been observed in nonlinear optical systems [1]. The construction in Fig. 1(b) was proposed [2] to characterize these states, but no explanation was provided for the physical origin of the wave number, k_d, needed to complete the resonant triads depicted in Fig. 1(a). Later work [5,6] suggested that k_d could correspond to a number of possible linearly stable (damped) modes in this system.

Our experiments study parametrically excited nonlinear waves on the two-dimensional (2D) surface of a fluid. The unperturbed system is driven by a spatially uniform, temporally periodic vibration of the fluid layer of the form: $a_1\cos(m_1\omega t+\phi_1)+a_2\cos(m_2\omega t+\phi_2)$, where m_1, m_2 are mutually prime, odd, and even integers [7]. Details of the experimental system can be found in [4]. We label the driving frequency ratio by m_1/m_2. Note that this differs from the $n_1:n_2$ labeling used to characterize grid states. The bulk of our quantitative measurements were performed at the frequency ratio $m_1/m_2=6/7$ although the grid states in Fig. 3 have also been observed for 8/9 driving. The experiments were performed in a 150-mm-diam cell filled with 18cS silicone oil at 31.5±0.05 °C, $\omega/2\pi=14$ Hz and, unless otherwise stated, a fluid depth, h, of 0.3 cm. Our experiments are in a dissipative regime, as $k_c\sqrt{\nu/\omega}\sim O(1)$. Due to both the large aspect ratio (typically $40-50\lambda_c$) and the dissipative nature of the fluid, the results described are independent of the system's lateral boundaries [7].

When the driving frequency is $m\omega$, the system's dominant temporal response is $m\omega/2$. The parity of the integer m plays an important role in determining the allowed types of nonlinear interactions. One can see this by performing a temporal translation of one driving period, $t\rightarrow t+2\pi/\omega$. This changes the sign of the linear modes when m is odd but

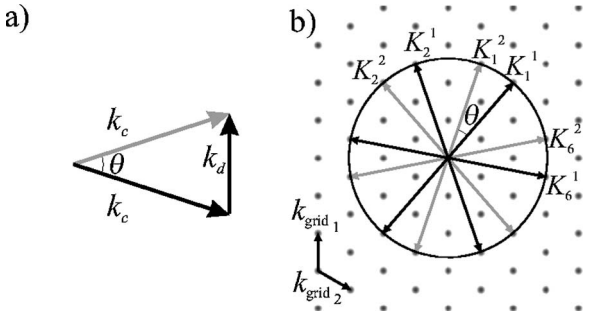

FIG. 1. (a) Three-wave interactions of corotated sets of critical wave numbers $\vec{K}_i$ ($|\vec{K}_i|=k_c$) coupled to a linearly damped wave number, $\vec{k}_d$, are (b) spanned by a sublattice of stable wave numbers, $\vec{k}_{grid_i}$ to form grid states.

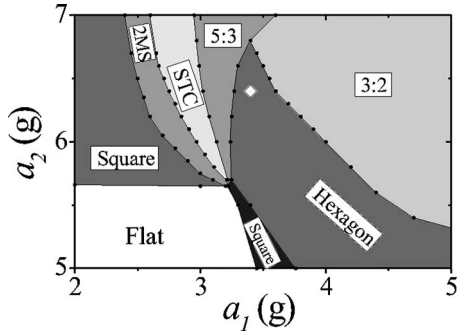

FIG. 2. Unperturbed phase diagram for 6/7 forcing for $h=0.3$ cm. To the right of the bicritical point at $(a_1,a_2)=(3.22,5.65)$ the phase space is dominated by quadratic interactions, where the 3ω mode (parametrically driven by 6ω) is linearly unstable. In this region we observe two types of grid states—3:2 [Fig. 3(a)] and 5:3 [Fig. 3(c)]. The two-mode superlattice (2MS) [4] is in the region dominated by the odd frequency, 7ω. Between these two regions a spatiotemporal chaotic state (STC) [4,10] exists. ◇ denotes the point $(a_1,a_2)=(6.4,3.4)$, where the measurements described in Fig. 4 were performed.

leaves them unchanged when m is even. As the system should be invariant under this action, quadratic nonlinearities are only allowed for even values of m. Thus, when m is *even* (*odd*) the dominant nonlinear self-interaction is quadratic (cubic). Similar considerations [8] limit the parity of the temporal mode corresponding to k_d [see Fig. 1(a)] to be even. Therefore, our choice of the forcing function enables us to select the dominant nonlinear interactions between modes.

To the unperturbed driving function (Fig. 2) we now add a small-amplitude perturbation of the form: $a_3\cos(m_3\omega t+\phi_3)$, where $m_3=2,4,5,8$ were used. Values of a_3 used were small, 20%–35% of the critical acceleration, $a_{3_{crit}}$ for exciting a linear mode at frequency $m_3/2$. A third frequency perturbation had previously been used in this system to stabilize both triangular [9] and quasicrystalline [4] patterns. In addition, the temporal parity of the perturbing frequency was utilized [10] to control spatiotemporal chaos formed by competing nonlinear states having different temporal parities. Here we use the *phase* of the third frequency to control the strength of quadratic interactions, and thereby select different types of nonlinear states.

We have observed *all* of the three types of grid states (3:2, 4:3, 5:3) possible up to $n_1=5$ (Fig. 3). A summary of their rotation angle θ and the damped wave number k_d is presented in Table I. Note that for the 3:2 and 5:3 states $k_d=k_{grid}$, while $k_d=2k_{grid}$ for the 4:3 grid states. The high-amplitude peaks on the inner circle of each spatial spectrum correspond precisely to the values of k_d defined by Eq. (2). This elucidates the physical significance of these modes, since the geometrical construction in Eqs. (1) and (2) contains no information about the relative amplitudes of different linear combinations of $\vec{k}_{grid_{1,2}}$. The time dependence of each of these grid states is an even multiple (harmonic) of ω, despite the fact that the driving contains an odd-parity frequency (7ω). Thus, in this region of phase space the major role of the odd-parity driving component is to enable quadratic interactions [7].

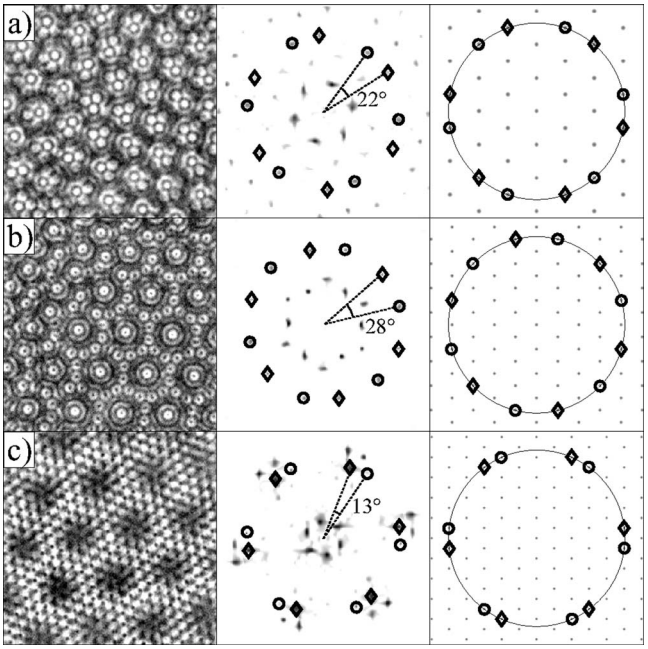

FIG. 3. (a) 3:2, (b) 4:3, and (c) 5:3 grid states. The spatial spectra (center) corresponding to the photographs (left) are spanned by grids (right) whose basis vectors, $\vec{k}_{grid}$, are stable modes. Fluid parameters are as in Fig. 2. Fluid depths: (a) and (c) 0.3 cm and (b) 0.2 cm. ◇ and denote corotated sets of $\vec{K}_i$.

Whereas only variants of the 3:2 grid state had been noted previously (coined "SL1" for 6/7 driving [3] and "DHS" for 2/3 driving [4]), the existence of the 4:3 and 5:3 states suggests the generality of grid states. These states all appear in the same region of phase space, where 5:3 grid states [Fig. 3(c)] were the most commonly observed. This state, predicted by [5] for different forcing parameters, appeared for all $6/7/m_3$ frequency ratios tested. The 3:2 state [Fig. 3(a)] was observed for $h=0.3$ cm for the majority of frequency ratios. This state was replaced by the 4:3 state [Fig. 3(b)] when the system dissipation was effectively increased by decreasing h to 0.2 cm.

At first glance, the 4:3 grid state could be mistaken for a 12-fold quasicrystalline pattern. The 28° rotation angle of the 4:3 state is close to the 30° angle expected for the 12-fold state, as suggested in [11]. A careful inspection of its higher spatial harmonics, however, reveals a clear differentiation between these two qualitatively different states.

Let us now turn to the selection of the different grid states. Recently, [6] investigated how the strength of these resonant triad interactions (Fig. 1) depends on the forcing

TABLE I. Predicted and observed values of the rotation angles $(\theta_{pred},\theta_{obs})$ and damped wave numbers (k_{d-pred},k_{d-obs}) of observed grid states.

n_1:n_2	θ_{pred}	θ_{obs}	k_{d-pred}	k_{d-obs}
3:2	21.8°	22°	$k_c/\sqrt{7}\sim 0.38k_c$	$0.38k_c\pm 0.02k_c$
4:3	27.8°	28°	$2\cdot k_c/\sqrt{13}\sim 0.56k_c$	$0.55k_c\pm 0.02k_c$
5:3	13.2°	13°	$k_c/\sqrt{19}\sim 0.23k_c$	$0.23k_c\pm 0.01k_c$

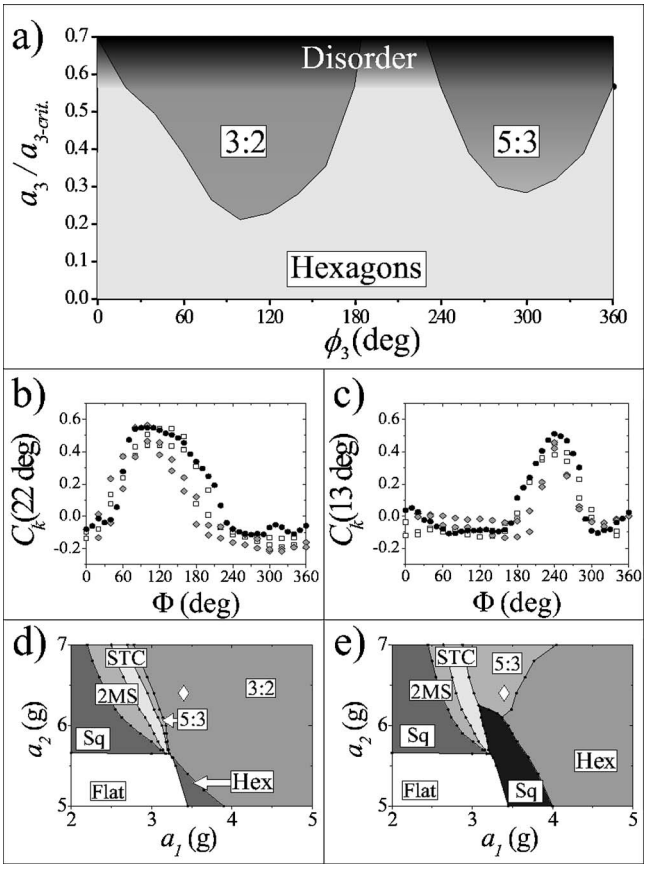

FIG. 4. (a) a_3, ϕ_3 phase diagram for 6/7/2 forcing at the point depicted by ◇ in Fig. 2. The generalized phase, Φ, selects the different grid states shown in (a). Angular correlation amplitudes at k_c of (b) the 3:2 phase at $\theta=22°$ and (c) the 5:3 phase at $\theta=13°$. Three different schemes were used to vary Φ; we first held $\phi_2=\phi_3=0$ and changed ϕ_1 by 20° jumps. We then used two cyclic permutations of this scheme. □$-\phi_1$, ◆$-\phi_2$, and •$-\phi_3$, used to calculate Φ collapse onto the same curve. (e) and (f) are phase diagrams of the perturbed system with $a_3=0.4a_{3_{crit}}$ where $\phi_3=90°$ and $\phi_3=270°$, respectively.

parameters of this system. This symmetry based analysis, predicted that the relative phases, ϕ_i, of the forcing terms may be used to enhance or suppress nonlinear interactions between two K_i vectors and the damped linear modes, k_d, which correspond to frequencies which are even multiples of ω [8]. For each $m_1/m_2/m_3$ forcing, a generalized phase, Φ, which is a specific linear combination of the ϕ_i, was shown to control the nonlinear coupling between these modes. Using the quasipotential model [12] for parametrically excited surface waves, selection of the 3:2 grid state as a function of Φ was demonstrated for systems with low dissipation.

The influence of the driving phases on the selection of nonlinear states is demonstrated in the a_3, ϕ_3 phase diagram presented in Fig. 4(a). For the values of $a_1=3.4$ g and $a_2=6.4$ g used (denoted by the diamond in Fig. 2), the system is in a pure hexagonal state for $a_3=0$. As a_3 is increased, surprisingly, two distinct regions of 3:2 and 5:3 grid states appear for $a_3 \sim 0.2a_{3_{crit}}$ and $a_3 \sim 0.3a_{3_{crit}}$ in the respective vicinities of $\phi_3=90°$ and $\phi_3=270°$. Beyond $a_3=0.6a_{3_{crit}}$ a transition to spatiotemporal chaos is observed. For driving

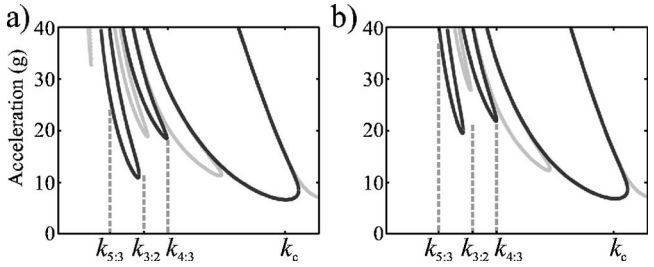

FIG. 5. Linear stability curves for $h=0.3$ (a) and 0.2 cm (b) with the other system parameters as in Fig. 4. Dark (light) lines depict even-parity (odd-parity) modes. $k_{n_1:n_2}$ is the wave number of the damped mode of a n_1:n_2 grid state.

ratios of 6/7/4 and 6/7/8 both the 5:3 and 3:2 grid states are also observed with a_3, ϕ_3 phase diagrams qualitatively similar to Fig. 4(a) but with different values of ϕ_3 at transition.

In [6] the strength of the nonlinear cross-coupling interactions was predicted to depend on both the generalized phases, Φ, and values of m_3. A quantitative measure of the strength of these interactions can be obtained by the use of the angular correlation function [4,13]

$$C_k(\theta) = \frac{\sum_\alpha [(f_k(\theta) - \bar{f}_k)(f_k(\theta+\alpha) - \bar{f}_k)]}{\sum_\alpha [(f_k(\alpha) - \bar{f}_k)^2]}, \qquad (3)$$

where $f_k(\alpha)$ is the power of the wave number k at the polar angle α. As grid states have a high degree of correlation at distinct angles θ, both the locations and amplitudes of peaks of the function $C_k(\theta)$ provide a quantitative measure of both the existence and stability of a given grid state.

To test the dependence of the cross-coupling strength as a function of Φ, we measured the Φ dependence of $C_{k_c}(22°)$ [Fig. 4(b)] and $C_{k_c}(13°)$ [Fig. 4(c)] for 6/7/2 driving. For this driving ratio, the predicted combination of ϕ_i comprising Φ is $\Phi=2\phi_1-2\phi_2+\phi_3$. Only when plotted as a function of this predicted combination for Φ, was a clear collapse of the data obtained [14]. In addition, the explicit value of $\Phi \sim 90°$ theoretically predicted by [6] for the peak value of the 3:2 grid state was observed. No special behavior, however, was predicted for the value $\Phi \sim 270°$, for which the 5:3 grid state was observed for the same forcing parameters [Fig. 4(c)]. Similar measurements were performed for 6/7/5 using $\Phi=2\phi_1-\phi_2-\phi_3$. Both frequency ratios yielded convincing collapses of the data with the above values of Φ. Φ in the latter case was predicted for $m/n/(2m-n)$ driving [6], but was not expected for 6/7/5 driving. This collapse may be due to high-order terms [15] not included in [6].

We have seen that the generalized phase, Φ, plays a significant role in the selection of nonlinear states. Φ is defined only by the temporal forcing ratios and, as demonstrated by Fig. 4, multiple grid states can be stabilized for the same forcing ratio. The explicit nature of a grid state, however, is determined by the value of k_d selected by the system.

The linearly damped modes are calculated for the parameters of Fig. 4 [16] in Fig. 5(a). For $6/7/m_3$ forcing ratios there are five linearly damped minima with wave numbers

smaller than the excited ones. The damped modes with even parity correspond to dominant response frequencies of ω and 2ω, whereas those of odd parity to $\omega/2$, $3\omega/2$, and $5\omega/2$. Symmetry considerations [8] allow only the even-parity modes to couple to two $\vec{K}_i$ modes. Later work [5] predicted that modes corresponding to the difference frequency, $|m_1-m_2|\omega$, the sum frequency, $(m_1+m_2)\omega$, and $m_i\omega$ should have the largest contribution to the coupling coefficient. As seen in Fig. 5(a), the wave number $k_{3:2}$ is indeed close to the critical wave number corresponding to ω.

When h is reduced from 0.3 to 0.2 cm, the 4:3 grid state *replaces* the 3:2 grid state at $\Phi=90°$. The selection of the 4:3 grid state may possibly be understood by examination of the linear stability diagram, Fig. 5(b), for $h=0.2$ cm. The change in h precipitated both an increase, by nearly a factor of 2, in the height of the stability curve corresponding to ω and a significant shift of the value of $k(\omega)$ away from $k_{3:2}$. At the same time, the stability curve minimum corresponding to 2ω shifted close to the value of $k_{4:3}$. The 4:3 grid state may have been enhanced relative to the 3:2 state by these changes.

This selection criterion, however, does not apply to the selection of the 5:3 grid state. Although selection of this state is determined by the generalized phase Φ, Fig. 5(a) indicates that *no* minimum of an even-parity tongue is in the vicinity of $k_{5:3}$. The selection of this wave number might be explained by the existence of an additional three-wave spatial resonance. For this grid state $\vec{k}_c+\vec{k}_d=\vec{k}_2$, where k_2 is the wave number of the linearly unstable (odd-parity) mode that corresponds to 7ω forcing. Although this resonance violates temporal parity (as no odd-parity temporal frequency is observed for the 5:3 state), we speculate that this second spatial resonance may be the key for understanding the selection of this state.

In summary, we have shown that *all* superlattice states generated by quadratic nonlinearities, in this system, are grid states. Although each specific grid state may be explained by a different mechanism, the important point here is that the spatial resonances inherent in these states appear to increase their stability. We have also demonstrated that both generalized phases, predicted by symmetry arguments, and intelligent selection of the system parameters can be used to select which grid states are created. As both quadratic nonlinearities and the above symmetry arguments are generic, we expect that these results should be relevant to a wide class of nonlinear systems. Indications of this can be seen in reanalysis of superlattice states observed in optical systems [1], where both the predicted angles and corresponding values of k_d consistent with a number of grid states are observed.

This research was supported by the Israel Science Foundation (Grant No. 194/02).

[1] E. Pampaloni, S. Residori, S. Soria, and F. T. Arecchi, Phys. Rev. Lett. **78**, 1042 (1997).
[2] M. Silber and M. R. E. Proctor, Phys. Rev. Lett. **81**, 2450 (1998).
[3] A. Kudrolli, B. Pier, and J. P. Gollub, Physica D **123**, 99 (1998).
[4] H. Arbell and J. Fineberg, Phys. Rev. Lett. **81**, 4384 (1998); Phys. Rev. E **65**, 036224 (2002).
[5] M. Silber, C. M. Topaz, and A. C. Skeldon, Physica D **143**, 205 (2000); C. M. Topaz and M. Silber, *ibid.* **172**, 1 (2002).
[6] J. Porter, C. M. Topaz, and M. Silber, Phys. Rev. Lett. **93**, 034502 (2004); C. M. Topaz, J. Porter, and M. Silber, Phys. Rev. E **70**, 066206 (2004).
[7] W. S. Edwards and S. Fauve, Phys. Rev. E **47**, R788 (1993); J. Fluid Mech. **278**, 123 (1994).
[8] M. Silber and A. C. Skeldon, Phys. Rev. E **59**, 5446 (1999).
[9] H. W. Muller, Phys. Rev. Lett. **71**, 3287 (1993).
[10] T. Epstein and J. Fineberg, Phys. Rev. Lett. **92**, 244502 (2004).
[11] A. M. Rucklidge and W. J. Rucklidge, Physica D **178**, 62 (2003).
[12] W. Zhang and J. Vinals, J. Fluid Mech. **341**, 225 (1997).
[13] F. Simonelli and J. P. Gollub, J. Fluid Mech. **199**, 471 (1989); D. Binks and W. van de Water, Phys. Rev. Lett. **78**, 4043 (1997).
[14] Similar results for the phase dependence (obtained in parallel to ours) are reported in Y. Ding and P. Umbanhowar, Phys. Rev. E **73**, 046305 (2006).
[15] J. Porter and M. Silber (private communication).
[16] T. Besson, W. S. Edwards, and L. S. Tuckerman, Phys. Rev. E **54**, 507 (1996).